Quantum router based on ac control of qubit chains

David Zueco,[1,*] Fernando Galve,[1,†] Sigmund Kohler,[2] and Peter Hänggi[1]

[1]*Institut für Physik, Universität Augsburg, Universitätsstraße 1, D-86135 Augsburg, Germany*
[2]*Instituto de Ciencia de Materiales de Madrid, CSIC, Cantoblanco, E-28049 Madrid, Spain*

We study the routing of quantum information in qubit chains. This task is achieved by suitably chosen time-dependent local fields acting on the qubits. Employing the physics of coherent destruction of tunneling, we demonstrate that a driving-induced renormalization of the coupling between neighboring qubits provides the key for controlling the transduction of quantum information between permanently coupled qubits. We employ this idea for building a quantum router. Moreover, we discuss the experimental implementation with Penning traps and study the robustness of our protocol under realistic experimental conditions, such as fabrication uncertainties and decoherence.

PACS number(s): 03.67.Bg, 75.10.Pq

I. INTRODUCTION

Entanglement, the inextricable quantum correlation between two physical objects is a key resource for quantum informational tasks which promise pushing further our current computational limits [1]. This resource, which is produced through the interaction of two (or more) quantum objects, needs to be created, used, and transferred under strict control such that a successful computation can be performed. Transporting entanglement may be considered as the analog of electric currents for classical computation, which need to be produced, then used for computation inside a CPU, and finally transferred to the output device.

In this paper we will focus on the process of transferring information once the computation has been performed. While long-distance quantum communication can be done quite efficiently with photons [2], communication inside a quantum computer will probably use linearly arranged solid-state qubits [3,4]. Lately, much attention has been paid to spin chains with nearest-neighbor coupling, which allow for perfect transfer of quantum information [5–9]. The simplicity of such chains and the fact that they do not require special control make them robust for experimental implementations [10]. It is our belief that a quantum computer will profit from more complicated devices which allow not only linear propagation but also the possibility to stop the signal at a given node in a network, reverse its motion, etc., such that the information can be *routed* to the desired node with minimal control. This could be particularly useful in quantum registers for storin, retrieving, and transfering information contained in different qubits.

The possibility of controlling the transfer in a spin chain is exciting. Such a chain could be used to inhibit access to parts of the register or even to divide a signal into two different branches for distribution in a network of nodes provided that a particular propagation direction can be chosen. At this point one could argue that for forbidding the propagation through a particular direction we "just need" to switch off the coupling in that direction [11]. However, coupling and decoupling qubits are a formidable task [12–15]. Therefore we should think of an alternative for breaking the symmetry and, thus, allowing the transfer in one direction without modifying the inter-qubit couplings.

The mathematics relating to coherent destruction of tunneling [16–18] or dynamical localization, i.e., the suppression of ballistic transport by ac fields [18–22] suitably solves the objective in the high-frequency limit [23]. Such driving renormalizes the tunnel matrix elements and has been investigated previously in the context of ac-driven mesoscopic transport [20,22,24]. In a recent theoretical work [25], it has been suggested to temporarily suppress tunneling between specific neighboring sites of an optical lattice, such that a particle will be transported into a direction of choice. Here we will demonstrate how to use such a dynamical renormalization for transmitting quantum information.

In Sec. II we introduce the concept of a *quantum router* and present in Sec. III an according chain model together with brief explanation of the coherent destruction of tunneling on which our quantum router relies. Section IV is devoted to the development of an according protocol for entanglement distribution and state transfer. A proposal for the implementation in Penning traps together with an analysis of the robustness of the method under experimental conditions is presented in Sec. V.

II. ROUTER FOR QUANTUM INFORMATION

Quantum information processing protocols usually depend on having full control of the qubits and their mutual interactions. This control relies on external devices such as lasers or signal generators, which limits the number of qubits by space considerations. One possible solution of this problem is applying quantum optimal control techniques to achieve quantum computation by acting on only a few number of qubits, leaving the rest evolve under the underlying and uncontrolled Hamiltonian [26–28]. Another possibility is splitting the processor into small blocks which, however, need to be connected [29]. Increasing the complexity of the network requires the selective coupling and decoupling of the blocks. We term a device that serves for this purpose

*david.zueco@physik.uni-augsburg.de
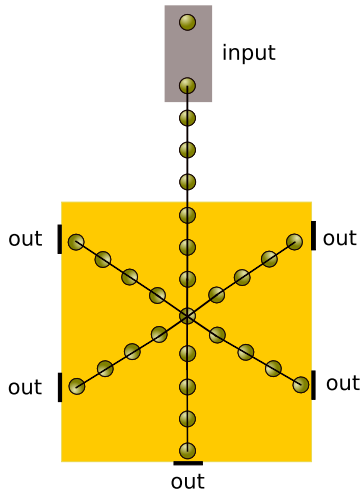†fernando.galve@physik.uni-augsburg.de

FIG. 1. (Color online) Hub configuration. One qubit of an entangled pair is connected to a line with perfect transfer. Then the entanglement propagates and is later steered to one of the possible outputs, i.e., distributed to the desired transmission line. This enables quantum communication inside the quantum computer by both direct state transfer and teleportation once the entanglement of distant parties has been established.

quantum router.

Let us assume for the moment that we have complete control of the coupling between every pair of qubits in an arbitrary array despite that fact that this requires quite sophisticated engineering, at least much more than the perfect unidirectional entanglement transfer described in Refs. [5–7]. Thus such a specialized piece of architecture is probably useful only for very specific tasks at particular points during computation, transfer, and storage. One example is the hub sketched in Fig. 1, let it be realized by a passive or an active element. When entanglement arrives at the junction, it should be routed to an output of choice. The output channel may either be selected by the router itself or depend on an additional classical signal containing that information. Moreover, the router may select the output direction by the time at which the signal arrives at the hub. This means that the hub effectively opens the channels in turns and delivers the signal accordingly.

A main obstacle for the experimental realization of a router is that it might be difficult if not impossible to simply turn off the interaction between neighboring qubits. Still, there exists an indirect way for this task that is based on the physics of "coherent destruction of tunneling." Let us consider a chain of qubits with given qubit-qubit interaction determined by the experimental setup. But nevertheless there exists the possibility of controlling the energy splitting of each qubit, which is typically less demanding than controlling the coupling. Then, as we will demonstrate below, an ac field with proper amplitude and frequency acting on the qubit will effectively renormalize the qubit-qubit interaction. It is even possible to suppress this interaction almost entirely. After explaining the underlying mechanism, we apply the idea to the T-shaped setup sketched in Fig. 2, where Alice sends a quantum state through the horizontal quantum channel. When the state arrives at the node, it shall be directed either
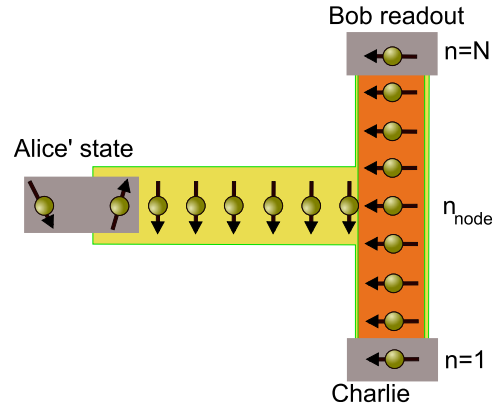

FIG. 2. (Color online) T-shaped configuration. Alice sends the state of one of her qubits without dispersion along the horizontal chain. When the state arrives at the node, an ac field with a ratchetlike profile transfers the signal to Bob or to Charlie.

to Bob or to Charlie. We demonstrate below that this can be achieved by applying to the qubit splittings of the vertical chain an ac control with a ratchetlike amplitude distribution.

Let us point out that our protocol is "cleaner" than other possibilities, such as bringing the spins out of resonance, which decouples them as well. This however is plagued with difficulties since parameter changes (in this case the local fields) usually lead to unwanted excitations. They become more likely the faster the parameters are changed. Thus one will spoil the entanglement unless the parameters are switched very slowly. Hence one would need to revert all such unwanted transitions, and thus, the process would become more difficult. Our protocol merely "renormalizes" the Hamiltonian without the disadvantages of directly changing the Hamiltonian itself. In this context it is worth mentioning two recent works which extend spin-chain engineering providing perfect transfer of Refs. [5,6] to directional state transfer in two-port architecture [30] and in a few qubit star network [31].

III. COHERENT DESTRUCTION OF TUNNELING IN CHAINS OF QUBITS

We consider entanglement transfer in the vertical qubit chain of Fig. 2 modeled by the Hamiltonian

$$H = \frac{1}{2}\sum_n h_n(t)\sigma_n^z + \frac{J}{4}\sum_n (\sigma_n^+ \sigma_{n+1}^- + \sigma_n^- \sigma_{n+1}^+), \quad (1)$$

with $\sigma_n^{\pm} = \frac{1}{2}(\sigma_n^x \pm i\sigma_n^y)$ and σ_n^{α}, $\alpha = x, y, z$ the usual Pauli matrices for spin n, while $\hbar = 1$. This Hamiltonian is known as the isotropic *XY* model with time-dependent local fields $h_n(t)$. The qubit-qubit coupling is a standard interaction realized either by direct engineering of the chain or as a rotating-wave approximation (RWA) where terms of the type $\sigma_n^+ \sigma_{n+1}^+$ and $\sigma_n^- \sigma_{n+1}^-$ are neglected [32–34]. Furthermore, we will see that the mechanism explained below can be observed as well in a bosonic chain of harmonic oscillators for which the Hamiltonian reads as

$$H = \frac{1}{2}\sum_n \frac{p_n^2}{m} + m\omega_n^2(t)x_n^2 + \lambda\sum_n x_n x_{n+1} \qquad (2)$$

provided a RWA in the coupling between the oscillators can be applied, i.e., neglecting the counter-rotating terms $a_n a_{n+1}$ and $a_n^\dagger a_{n+1}^\dagger$ [35].

We assume that the onsite qubit splitting possesses a time dependence stemming from a classical field of the form

$$h_n(t) = A b_n \cos(\omega t). \qquad (3)$$

In the interaction picture defined by $\widetilde{X} = U_0^\dagger(t) X U_0(t)$, where $U_0(t) = \exp[-i\varphi(t)\sigma_z]$ and $\dot{\varphi}(t) = h_n(t)/2$, Hamiltonian (1) reads as

$$\widetilde{H}(t) = J\sum\; e^{i\eta_n(t)}\sigma_n^+\sigma_{n+1}^- + e^{-i\eta_n(t)}\sigma_n^-\sigma_{n+1}^+, \qquad (4)$$

with the phase

$$\eta_n(t) = \frac{A}{\omega}(b_n - b_{n+1})\sin(\omega t). \qquad (5)$$

In the high-frequency limit $\omega \gg J$, the interaction-picture Hamiltonian (4) can be replaced by its time average. Thus, we obtain an effective static *XY* chain Hamiltonian for which the coupling between qubits n and $n+1$ is renormalized according to

$$J \to J_{\mathrm{eff},n} = J J_0\!\left(A\frac{b_n - b_{n+1}}{\omega}\right), \qquad (6)$$

where J_0 denotes the zeroth-order Bessel function of the first kind. Thus, the coupling between sites n and $n+1$ can be tuned to zero by choosing driving parameters for which $A(b_n - b_{n+1})/\omega$ is a root of J_0. This renormalization has been used to explain the phenomenon of coherent destruction of tunneling [16–18,36]. Here we use it to steer quantum information by temporarily suppressing the interaction between two particular spins.

IV. PROTOCOLS AND CONTROL MECHANISM

Quantum routers may be useful for various purposes. We focus in the following on two of them, namely, entanglement distribution and quantum state transfer. We develop for these aims protocols that rely on the coherent destruction of tunneling (CDT) mechanism introduced in the previous section. It will turn out that both protocols are closely related.

A. Entanglement routing

An essential resource for quantum communication is a pair of distant entangled qubits, one at each end of the communication channel [37]. Such pairs can be obtained by creating the entangled pair locally and subsequently transfer to each end one partner. Recently, Creffield suggested to use the CDT mechanism described above for the controlled coherent propagation in a lattice [25]. Different to this entanglement transfer is the previously suggested nonlocal creation of entanglement in a spin chain [38,39].

The topic of this subsection, by contrast, is to create an entangled pair at Alice's place and to route one partner to either Bob or Charlie, see Fig. 2. A possible protocol for this task is the following: let Alice have a two-qubit entangled state $|\psi\rangle_A$ that she wants to share with Bob. She will then attach one of the qubits to a chain with isotropic nearest-neighbor interaction such that the qubit propagates toward the node with the vertical chain. If she, for example, owns the state $|\psi(0)\rangle = (|01\rangle + |10\rangle)/\sqrt{2}$, the horizontal chain has the initial state

$$|\psi\rangle_{\mathrm{in}} = \frac{1}{\sqrt{2}}(|1\rangle_A|00\cdots00\rangle + |0\rangle_A|10\cdots00\rangle), \qquad (7)$$

while the desired final state is

$$|\psi\rangle_{\mathrm{out}} = \frac{1}{\sqrt{2}}(|1\rangle_A|00\cdots00\rangle + |0\rangle_A|00\cdots01\rangle). \qquad (8)$$

Such perfect entanglement transfer can be achieved by specific static couplings [5–7]. The question is now whether time-dependent fields allow one to route the qubit in a controlled manner from the node of the T junction to either Bob or Charlie.

When the traveling qubit arrives at the node of the T junction (see Fig. 2), coherent destruction of tunneling must become active such that propagation to, say, Charlie's branch is suppressed. Our goal is now to find an ac field such that the entanglement is perfectly transmitted to Bob. Moreover, the protocol should be flexible enough to allow routing to Charlie as well.

We consider now a qubit chain that consists of blocks with four qubits with the ratchetlike energy splittings [40,41]

$$b_n = \begin{cases} b, & n = 4n' \\ b + \Lambda_1, & n = 4n' + 1 \\ b + \Lambda_1 + \Lambda_2, & n = 4n' + 2 \\ b + \Lambda_2, & n = 4n' + 3 \end{cases} \qquad (9)$$

for integer n', as is sketched in Fig. 3(a). It is constructed such that the energy differences between two neighboring qubits are given by the sequence $\Lambda_1, \Lambda_2, -\Lambda_1, -\Lambda_2$, i.e., their absolute values alternate between Λ_1 and Λ_2. CDT can now be employed for temporarily suppressing tunneling between qubits with the one or the other value of the splitting [note that $J_0(-x) = J_0(x)$, such that the CDT condition is not sensitive to the sign of $\Lambda_{1,2}$]. A field that alternates between these two possibilities can induce directed transport [25]. We here use this idea to route entanglement. To be specific, we act on qubit n the driving field

$$h_n(t) = \xi_0\omega b_n \cos(\omega t)\begin{cases} 1/\Lambda_1, & 0 \le t < T_1 \\ 1/\Lambda_2, & T_1 \le t < T_1 + T_2 \end{cases} \qquad (10)$$

and periodically continued [see Fig. 3(b)] where $\xi_0 = 2.4048\ldots$ is the smallest positive root of the Bessel function J_0. For this field, the CDT condition $J_{\mathrm{eff}} = 0$ is fulfilled for the transitions $4n' \leftrightarrow 4n'+1$ and $4n'+2 \leftrightarrow 4n'+3$ during the time interval $[0, T_1]$, while the other transitions are still allowed. For them the effective coupling energy is $J_{\mathrm{eff},1} = J J_0(\xi_0\Lambda_1/\Lambda_2)$. The length of the time interval,
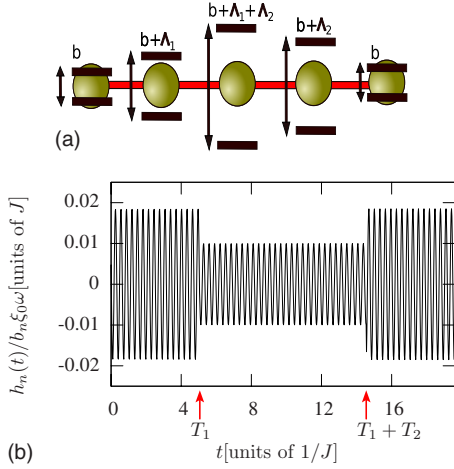
FIG. 3. (Color online) (a) Spatial variation in the local qubit energy splittings along the vertical chain. It is chosen such that the absolute value of differences between two neighboring sites alternates between Λ_1 and Λ_2. (b) Ac field with alternating driving amplitude. The amplitudes [see Eq. (10)] are such that tunneling between qubits with either energy difference Λ_1 or Λ_2 is suppressed.

$T_1 = \pi / |J_{\mathrm{eff},1}|$, corresponds to a half tunnel cycle between qubits $4n'$ and $4n'+1$, such that these qubits exchange their state. During time interval $[T_1, T_1+T_2]$, we obtain that the coupling between spins with energy difference Λ_2 is suppressed, while the other coupling is renormalized according to $J_{\mathrm{eff},2} = J J_0(\xi_0 \Lambda_2 / \Lambda_1)$. Thus the second stage has to last for $T_2 = \pi / |J_{\mathrm{eff},2}|$.

Next, we test numerically the quality of the entanglement transfer. Since the isotropic *XY* model conserves the number of excited spins, it is sufficient to consider only the subspace with at most one qubit in state 1, while all other qubits are in state 0. Then the chain can be mapped to the tight-binding model

$$H = \sum_n h_n(t) |n\rangle\langle n| + \frac{J}{2} \sum_n (|n\rangle\langle n+1| + |n+1\rangle\langle n|), \quad (11)$$

with the $(N+1)$-dimensional state vector

$$|\psi(t)\rangle = \sum_{n=0}^{N} c_n |n\rangle, \quad (12)$$

where $|n\rangle = |0\rangle_A |00\cdots 1_n \cdots 00\rangle$ denotes the state in which the *n*th qubit of the chain is the only one in state 1. In order to achieve a compact notation, we have introduced the state $|0\rangle = |1\rangle_A |0\cdots 0\rangle$ for which all qubits are in the ground state, while Alice' state is excited.

The main requirement for our protocol is that Alice's qubit remains entangled with the qubit that propagates to Bob or to Charlie, respectively. We measure this property by the concurrence $C = \max\{\lambda_1 - \lambda_2 - \lambda_3 - \lambda_4, 0\}$ [42]. The λs are the ordered square roots of the eigenvalues of the matrix $\rho(\sigma_y^1 \otimes \sigma_y^2)\rho^*(\sigma_y^1 \otimes \sigma_y^2)$, with ρ being the reduced density matrix of the considered qubit pair. In our case, the relevant reduced density matrix is that of Alice's qubit and qubit *n* of the chain. Tracing out all other qubits, we obtain in the basis $\{|0_A 0_n\rangle, |0_A 1_n\rangle, |1_A 0_n\rangle, |1_A 1_n\rangle\}$ the expression
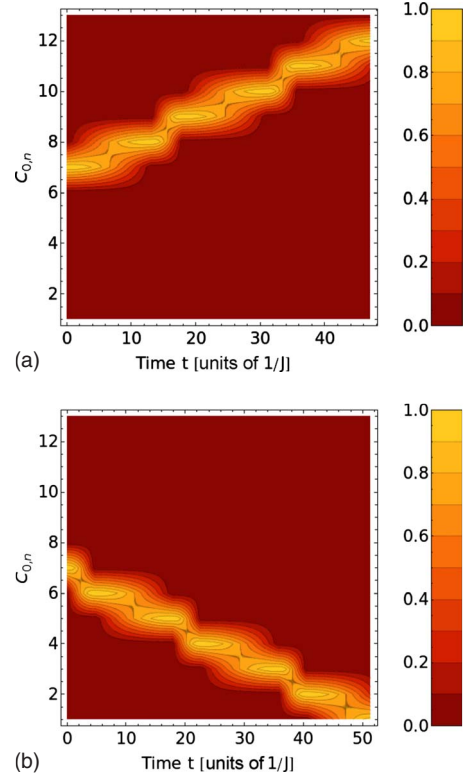

FIG. 4. (Color online) (a) Time evolution of the concurrence between Alice's qubit and qubit *n* of the vertical chain with length $N=13$ for the parameters $\omega=10J$, $b=J$, $\Lambda_1=3J$, $\Lambda_2=1.5J$. Alice' qubit is initially entangled with the qubit at $n_{\mathrm{node}}=7$. The onset of the driving field [Eq. (10)] is such that initially transfer to Charlie is suppressed. (b) Same as panel (a) but for an arrival time $t=T_1$ at the node, such that the entanglement propagates to Charlie.

$$\rho_{A,n} = \begin{pmatrix} \sum_{i\neq 0,n} |c_i|^2 & 0 & 0 & 0 \\ 0 & |c_0|^2 & c_n^* c_0 & 0 \\ 0 & c_0^* c_n & |c_n|^2 & 0 \\ 0 & 0 & 0 & 0 \end{pmatrix} \quad (13)$$

for which the concurrence reads as

$$C_{A,n} = 2|c_0 c_n|. \quad (14)$$

If Alice transfers her qubit directly to the node, i.e., to the central qubit n_{node} of the vertical chain, we can start our numerical calculation with the initial state

$$|\psi(0)\rangle = \frac{1}{\sqrt{2}}(|0\rangle + |n_{\mathrm{node}}\rangle). \quad (15)$$

Figure 4 shows the corresponding time evolution of the concurrence $C_{A,n}$. It demonstrates that for a proper onset of the driving field [Eq. (10)], the entanglement propagates solely to Bob who finally receives a state that is perfectly entangled with Alice's state. For a driving field starting with the larger of the two amplitudes, the entanglement propagates equally perfectly to Charlie, see Fig. 2. Thus, one can route the entanglement to a particular end of the vertical chain by choosing a proper initial time of the driving field.
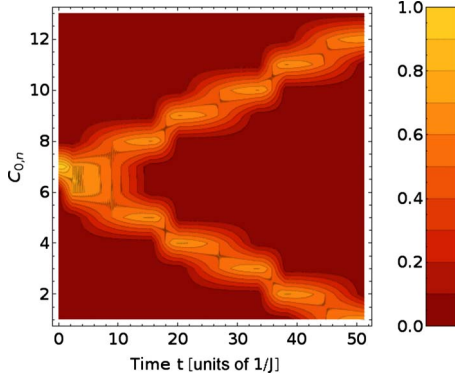
FIG. 5. (Color online) Same as Fig. 4 for the arrival time $t = T_1/2$ at the node, such that the traveling qubit is split.

It is also possible that both Bob and Charlie receive a state that is entangled with Alice's state as can be appreciated in Fig. 5. There the traveling qubit arrives with a delay of $t = T_1/2$, such that the routing toward Bob is only half completed at the time the upward channel is closed and routing to Charlie begins.

So far we have only discussed the dynamics in the vertical chain. The reason was that we are interested in the steering of the entanglement to Charlie or Bob once the entanglement arrives at the vertical chain. On the other hand, one could worry about possible dynamical reflections in the connection node. Intuitively the reflection can be associated with a change in the sound velocity between the two branches. On the other hand, for equal coupling constants between the connection node and the corresponding neighbors in the horizontal and vertical chains no reflection is expected. To confirm this picture we plot in Fig. 6 the full dynamics taking into account both the horizontal and vertical line. For the horizontal chain we assume also the isotropic *XY* model (1) with homogeneous qubit-qubit coupling. The effective coupling [Eq. (6)] between the central node and its neighbor in the vertical chain is chosen to be the same as the one in the
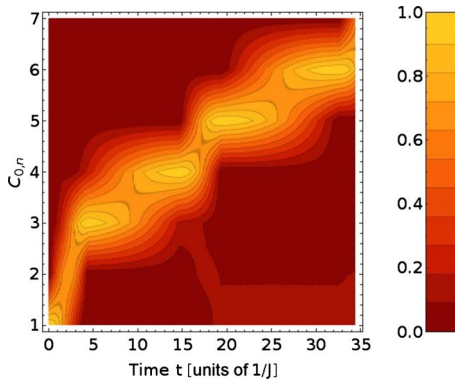

FIG. 6. (Color online) Study of dynamical reflection of entanglement at the entrance of the router (joint between horizontal and vertical lines in Fig. 2). The amount of entanglement is given by the concurrence, see Eq. (14). Here the horizontal chain is formed by the first two qubits and the rest is router, with the same parameters as in Fig. 4; a slight reflection is seen, but the transmitted entanglement lies above 0.98.
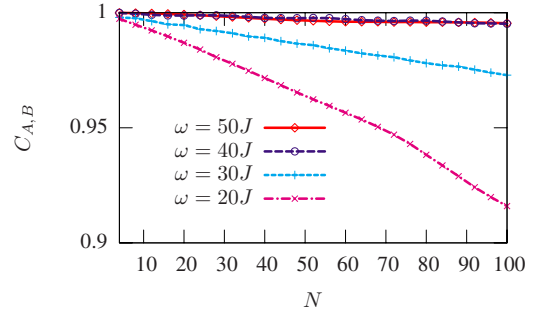

FIG. 7. (Color online) Length dependence of the final concurrence for chains of various frequencies. The differences of the energy splittings are $\Lambda_1 = 100J$ and $\Lambda_2 = 59.02J$, corresponding to the ratio $\Lambda_2/\Lambda_1 = 0.5902$ which provides the optimum transfer velocity.

horizontal line. However and due the different dynamics in both branches some entanglement is lost in the dynamics between the third and fourth nodes. In any case the transmitted concurrence lies above 0.98.

Our intuition for the dynamics of the quantum router is based on the derivation of an effective time-independent Hamiltonian derived within high-frequency approximation. In the following we numerically test the results of our high-frequency approximation for finite driving frequencies. In Fig. 7 we plot the final concurrence $C_{A,B}$ of Alice's qubit and the qubit that Bob receives for different driving frequencies. We find that the protocol works provided that the driving frequency is sufficiently large. For chains of length up to $N = 100$, the final entanglement is quite large, e.g., $C_{A,B} \gtrsim 0.97$ for $\omega \gtrsim 30J$. For driving frequencies $\omega \lesssim 20J$, the concurrence already assumes a significantly lower value.

In Fig. 7, we used a driving field with the amplitude ratio $\Lambda_1/\Lambda_2 = 0.5902$ for which the entanglement transfer is as fast as possible for a given value of J. Then the operation time and, thus, the total coherence loss are kept to a minimum, see subsection V 2. In order to obtain the optimized amplitude ratio, one has to consider that during a full cycle of the driving field, the entanglement is transported over two sites. This takes the time

$$T_1 + T_2 = \frac{\pi}{2|J_0(\Lambda_1/\Lambda_2)|} + \frac{\pi}{2|J_0(\Lambda_2/\Lambda_1)|}, \quad (16)$$

which possesses a minimum for the mentioned ratio and for the inverse ratio as well.

B. Quantum state transfer

The spin chain can also be used for quantum state transfer, such that a classical communication channel becomes dispensable [3]. For investigating state transfer, we assume that Alice owns the state

$$|\psi\rangle_A = \alpha|0\rangle + \beta|1\rangle, \quad (17)$$

which she likes to transfer to Bob. In doing so, she initializes the chain with the first qubit in the target state, while the other qubits of the horizontal chain are set to the ground state. For an excitation-preserving spin chain such as the one

defined by Hamiltonian (1), it can be shown that the unitary evolution of the chain provides Bob with the state [4]

$$\rho_B = \begin{pmatrix} 1 - |\beta|^2 |c_B| & \alpha\beta^* c_B \\ \alpha^*\beta c_B & |\beta|^2 |c_B| \end{pmatrix} \quad (18)$$

written in the basis $\{|0\rangle, |1\rangle\}$. Perfect state transfer corresponds to $|c_B| = 1$. For our driven spin chain with different local qubit splittings and ac fields, each transfer from one qubit to the next contributes a particular phase shift. Thus, Bob will receive a state with $c_B = |c_B| e^{i\theta}$. In order to restore the full state [Eq. (17)], one has to know the total phase shift θ, which requires full knowledge of the transfer process, i.e., one has to calibrate the chain before use. Subsequently, a fixed unique phase shift has to be applied to every signal coming from the hub. Such hub together with a data sheet that contains the phase shifts could represent a useful piece of hardware.

Finally, the quality of the state transfer can be quantified with the fidelity

$$F = |\langle \psi_A | \rho_B | \psi_A \rangle|, \quad (19)$$

which in our case reads as

$$F = 1 - (1 - C_{A,B})|\beta|^2 [1 - C_{A,B}(1 - 2|\beta|^2)], \quad (20)$$

after the phase has been rotated back. This means that the fidelity directly relates to the concurrence, $C_{A,B}$ in Eq. (14), of the entanglement router.

V. PHYSICAL IMPLEMENTATIONS

A highly accurate and stable confinement of ions in traps has been achieved in the last decade, together with the possibility of working in the ground state of the ion motion [43,44]. This enables the realization of quantum chains that consist of harmonic oscillators with a nearest-neighbor coupling. The physical origin of the coupling can be Coulomb interaction between the confined particles or a capacitive coupling of the ions residing in neighboring wells; see, e.g., Refs. [32,33]. For a comprehensive review of according control and readout techniques, see Ref. [43].

The Hamiltonian for the excitations in Eq. (11), with a general onsite Zeeman field $h_n(t)$ can also be implemented by a chain of harmonic oscillators. The particular form of the interaction is typically obtained by coupling the spatial coordinates of neighboring oscillators [see Eq. (2)] as is the case for Coulomb interaction between charged particles in dipole approximation. Note however that the resulting Hamiltonian contains terms that create and annihilate phonon pairs. These terms vanish within rotating-wave approximation, which means that a mapping to our spin-chain model [Eq. (1)] is possible only if this approximation holds, i.e., if the coupling is much weaker than the time average of an applied "Zeeman" field, $J \ll h_0$, where here $h_n(t) = h_0 + b_n(t)$. Notice that the presence of the constant "Zeeman" field h_0 merely rescales the energies and will not affect the router otherwise. Experimentally, this field can be realized by an ac voltage with nonzero mean, such that $h_n(t) = 2\hbar\omega_n(t)$ with the frequency $\omega_n(t)$ proportional to the square root of the applied voltage.

As a particular example, we consider singly trapped ions in planar Penning traps, in which neighboring ions couple capacitively through a conducting wire. Neglecting resonant absorption in the wire, the coupling for a typical trap size of 1 mm will be roughly 100 times lower than the onsite potential [33]. For even smaller traps of size 0.1 mm, these quantities still differ by a factor of 10. Thus, engineering the coupling strength essentially means choosing the correct trap size. For planar traps, the ion can be moved further away from the electrodes, which reduces the coupling even more. In a linear array of trapped ions such as the one of Ref. [32], the atoms experience Coulomb interaction. In both cases, the ratio between interaction strength and onsite potential $\hbar\omega$ is proportional to $q^2/(\pi\epsilon_0 m\omega^2 d^3)$. The difference in strength between both approaches is a form factor due to the fact that the wire-mediated coupling has a given efficiency when transmitting Coulomb interaction. In the case of direct Coulomb interaction, the coupling is slightly stronger but can be reduced by pushing the ions far apart from each other because J is reciprocal to the typical distance between the ions.

It must be noted here that for Penning traps, all parameters basically depend on two scales, namely, the trap size and the voltage. The motional frequency is proportional to $\sqrt{V}/d$, where V is the applied voltage and d the size of the trap. Manipulating both scales allows one to achieve the desired parameter values.

Robustness under realistic conditions

In an experiment, one usually faces additional difficulties not captured by a Hamiltonian with perfectly stable parameters. Two such difficulties come to mind, namely, imperfections in the fabrication process and the unavoidable influence of an environment that causes dissipation and decoherence.

1. Fabrication uncertainties

An essential ingredient to our entanglement distribution protocol is the action of the onsite ac fields $h_n = b_n(\xi_0\omega/\Lambda_i)\sin\omega t$ during times $T_i = \pi/J_{\text{eff},i}$, with $J_{\text{eff},1(2)} = JJ_0(\xi_0\Lambda_{1(2)}/\Lambda_{2(1)})$ [see Eq. (10) and Fig. 3]. This implies two critical experimental requirements. First, the driving amplitudes have to match with good precision the first zero of the Bessel function, and second, the field amplitudes have to be switched after a time $T_{1,2}$.

Trap diameters in the submillimeter range, correspond to motional frequencies of the order GHz, with a $J \sim 100$ MHz, such that the rotating wave approximation is applicable. Moreover, a driving frequency of the order 0.1 GHz is available with current technology, while commercially available function generators at those frequencies can have an accuracy of several 10^9 samples per second. Thus the switching times can be adjusted with precision $\epsilon_T = 10^{-3}/J$. The uncertainty in J mostly comes from measuring the distance between trapped ions (typically by fluorescence). Assuming an accuracy of 10%, we obtain the error $\epsilon_J = 10^{-7}J$, which corresponds to $\epsilon_T = 10^{-7}/J$. Thus, the relevant restriction is the mentioned uncertainty in the function generator, such that $\epsilon_T = 10^{-3}/J$. Concerning the amplitudes, we assume a relative error in the applied confining voltages

of the order of 10^{-6}, which yields an amplitude uncertainty of the order of $10^{-7}J$.

For a numerical simulation of these errors, we choose for each coupling matrix element J_i a random value from the interval $[J - \epsilon_J, J + \epsilon_J]$ with equal distribution. The interval width $2\epsilon_J$ is determined by the experimental uncertainties discussed above. Accordingly, we select a field amplitude from the interval $[b_n - \epsilon_b, b_n + \epsilon_b]$. In the following, we denote ensemble averages of such realizations by an overbar.

We already emphasized in Sec. III that the protocol for entanglement transfer is closely related to the one for state transfer. The main difference is that the latter requires knowledge of the extra phase θ. It has to be gauged or determined from theoretical considerations, such that Bob is able to compensate this phase by a local transformation. When the system parameters acquire a random component, the extra phase becomes random as well.

In principle, the additional random phase can be compensated by local transformations. Thus, it cannot influence the entanglement. Numerically, we have tested that the experimental uncertainties mainly affect this phase, making the concurrence fairly independent of this type of errors. Therefore we focus on the impact of the fabrication uncertainties on the state transfer. Assuming that we can gauge our apparatus, we know that the actual value of $\theta = \bar{\theta} + \Delta_\theta$ deviates from the average by Δ_θ. Notice that $\bar{\theta}$ can be obtained just by averaging over many realizations, as we discuss below. Then the fidelity (19) becomes [cf. Eq. (20)]

$$F = 1 - |\beta|^2 (1 - 2C_{A,B} \cos \Delta_\theta + C_{A,B}^2) + 2|\beta|^4 C_{A,B} (C_{A,B} - \cos \Delta_\theta). \quad (21)$$

Thus, all the possible errors are captured by the phase deviation $\theta = \bar{\theta} + \Delta_\theta$.

Figure 8 shows the frequentness of the accordingly reduced values for the fidelity. We have computed the fidelity (19) for 500 realizations of the spin chain and plotted a histogram with bin size 10^{-3}. Obviously, the driving frequency $\omega = 30J$ yields in most cases a fidelity $F > 0.98$ [panel (a)]. For a larger driving frequency [panel (b)], the fidelity distribution is still peaked at a value larger than 0.99. The standard deviation, however, is quite large, such that significantly smaller fidelities become rather likely. Thus, fabrication uncertainties impose that the driving frequency should not exceed $30J$. On the other hand, we have seen in Sec. IV A that this value in fact also represents a lower bound for the validity of the rotating-wave approximation within which the effective coupling strength [Eq. (6)] has been derived. Thus, we conclude that the results are best for a driving frequency of the order $\omega = 30J$.

2. Dissipation and decoherence

Still we have to consider the main obstacle for any quantum information task, which is dissipation and decoherence caused by weak but unavoidable coupling of the processor to a typically huge number of uncontrollable degrees of freedom. Irrespective of its physical nature, the environment is usually modeled as a bath of harmonic oscillators, where
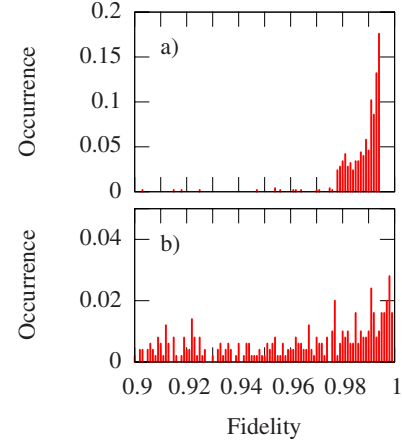

FIG. 8. (Color online) Fidelity distribution for the initial state $|\psi\rangle_A = (|0\rangle + |1\rangle)/\sqrt{2}$ in a chain with length $N = 40$ and the driving frequencies (a) $\omega = 30$ and (b) $\omega = 40$. The qubits splittings are $\Lambda_1 = 100J$ and $\Lambda_2 = 59.02J$, while the parameter uncertainties read $\epsilon_J = \epsilon_b = 10^{-7}$ and $\epsilon_T = 10^{-3}$. The data have been obtained from 500 realizations. The resulting standard deviations of the concurrence are 0.01 and 0.1, respectively.

each oscillator couples via its position operator to a system coordinate [18,45–47]. Here we assume that each qubit n undergoes pure and independent dephasing, i.e., that each coordinate σ_n^z couples to a separate bath.

For weak dissipation, one can eliminate the bath within second-order perturbation theory and derive a Bloch-Redfield master equation for the reduced density operator ρ of the qubits [48]. Considering, only phase noise on the traps the equation takes a Lindblad form [49]

$$\dot{\rho} = -\frac{i}{\hbar}[H, \rho] + \frac{\gamma}{2} \sum_{n=1}^{N} (\sigma_n^z \rho \sigma_n^z - \rho), \quad (22)$$

where we have assumed that the effective decoherence rate γ is the same for all qubits. Remarkably, such a master equation describes, apart from a transient, the decoherence process quite accurately [50]. For qubit arrays implemented with calcium ions confined in a Paul trap, the dephasing rate is $\gamma \sim 1$ kHz, while the qubit splitting is several MHz. The heating rate, which would include relaxation terms in the master equation, is 190 times smaller [51]. This justifies the phase noise model used here. We will use this numbers for a rather conservative estimate and assume $\gamma \sim 10^{-4}J$, where $J \sim 10$ MHz.

For qubit chains under the influence of phase noise, the entanglement decay is determined by the coherence loss, and one finds that the concurrence decays exponentially with a rate 2γ, i.e., $C_{A,B}(t) \propto \exp(-2\gamma t)$ [52]. This can be verified easily by considering the action of the dissipative kernel in the master equation on the off-diagonal density matrix elements $\rho_{nn'}$. The entanglement propagation from the middle of the chain to Bob's end takes the time $\tau_{AB} = (T_1 + T_2)N/4$ [Recall that our ratchet mechanism transports signals during a time $T_1 + T_2$ over two sites; see derivation of Eq. (16)]. Thus, we expect that decoherence reduces the finally achieved entanglement according to
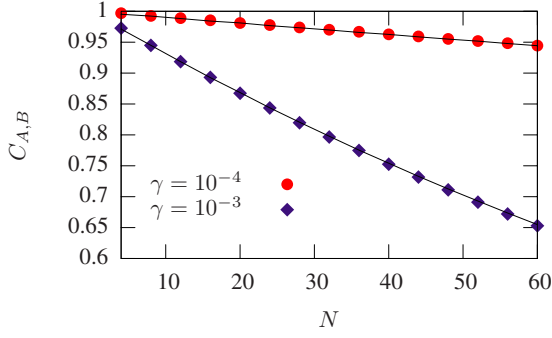
FIG. 9. (Color online) Concurrence decay as a function of the chain length for two different decoherence rates γ (symbols) and $\omega=30$. The solid lines mark the estimate [Eq. (23)]. All other parameters are as in Fig. 8.

$$C_{A,B} = C_{A,B}(\gamma=0)e^{-2\gamma\tau_{AB}}. \quad (23)$$

We numerically computed the time evolution described by the master equation (22). The results shown in Fig. 9 confirm our expectations for the exponential decay. Moreover, they demonstrate that a decoherence rate of $\gamma=10^{-4}J$ reduces the concurrence in a chain of length $N=60$ from $C_{A,B}(\gamma=0)=0.98$ in the absence of decoherence to a value $C_{A,B}=0.95$. This is still sufficiently large for most possible applications. For a larger decoherence rate, $\gamma=10^{-3}J$, however, the concurrence drops significantly. For example, in a chain of length $N=60$, we have the already quite small value $C_{A,B}=0.65$. Thus, we can conclude that for chains of this length, transmission of sufficient entanglement is only possible for decoherence rates that fulfill $\gamma \lesssim 10^{-4}J$. For stronger decoherence, a hub with shorter chains is nevertheless possible, in the extreme limit even one with branches that consist of just one qubit.

We close our analysis of fabrication uncertainties and decoherence by addressing also the fidelity of the state transfer protocol. In the presence of decoherence, it is no longer possible to establish an exact relation between the fidelity and the concurrence (20). The reason for this is that state transfer is limited by the dephasing of *individual* qubits, while the entanglement decay is influenced by the coherence between *different* qubits. The state transfer fidelity to Bob can still be expressed in terms of Bob's reduced density matrix [Eq. (18)] and now reads as

$$F = 1 - \rho_{11} + |\beta|^2(2\rho_{11} - 1) + 2|\rho_{10}|\text{Re}(\alpha\beta e^{i\Delta_\theta}), \quad (24)$$

which implies that again the average phase shift $\bar{\theta}$ plays a role; cf. Eq. (21).

We find numerically that the final population of Bob's qubit, which is described by the density matrix element ρ_{BB}, is practically independent of both the decoherence strength γ and the fabrication uncertainties. Without these influences, the state transfer protocol works almost perfectly, such that we can approximate this density matrix element by $\rho_{BB}=|\beta|^2$. Moreover, we already argued that off-diagonal matrix elements decay as $\rho_{B0}=\alpha\beta^* \exp(-\gamma\tau_{AB})$ and, thus, the finally achieved fidelity can be well approximated by
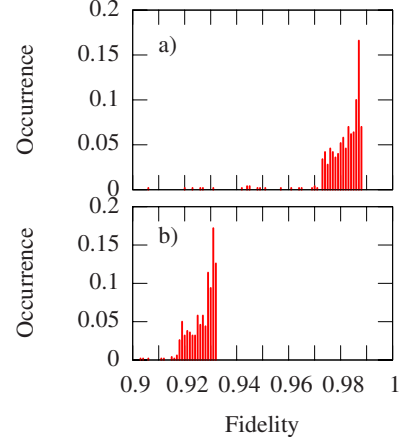

FIG. 10. (Color online) Fidelity spread for a chain of length $N=40$ with the initial state $|\psi\rangle_A=(|0\rangle+|1\rangle)/\sqrt{2}$. The driving frequency is $\omega=30$ and dissipation strengths (a) $\gamma=10^{-3}J$ and (b) $\gamma=10^{-4}J$. The histogram is obtained from 500 realizations yielding a standard deviation of 0.01 in both of them. All other parameters are as in Figs. 8 and 9.

$$F = 1 - 2(|\beta|^2 - |\beta|^4)[1 - \cos(\Delta_\theta)e^{-\gamma\tau_{AB}}]. \quad (25)$$

Thus, within some reasonable approximations, we again find for the fidelity a closed expression that is a function of the initial state. In fact, for $\gamma=0$ and $C_{AB}(\gamma=0)=1$, expression (25) becomes identical with the fidelity (21) for an ideal chain. This also demonstrates that the fidelity is significantly affected by both fabrication uncertainties and decoherence, expressed in Eq. (25) by the random phase shift Δ_θ and the exponentially decaying factor, respectively.

It remains to numerically corroborate the quality of the approximate result (25). Figure 10 depicts the numerical results for a chain of length $N=40$. It reveals that the maximum fidelity in the histogram coincides with making $\Delta_\theta=0$ in Eq. (25), namely, $F=0.99$ for $\gamma=10^{-4}J$ and $F=0.93$ for $\gamma=10^{-3}J$. Further the data spread due to the fabrication errors, is pretty the same that in the case without decoherence [cf. Fig. 8]. This underlines that state transfer with fidelity $F\gtrsim 0.97$ is achievable with the experimental realization discussed above, provided the dissipation rate does not exceed the value $\gamma=10^{-4}J$.

VI. DISCUSSION AND CONCLUSION

We have proposed a quantum router that can be employed for steering one qubit of an entangled pair from Alice to either Bob or Charlie. A second related application is quantum state transfer. With the experimental realization with ion traps in mind, we have presented analytical and numerical results that underline the feasibility of our scheme.

The underlying physics is coherent destruction of tunneling between two neighboring qubits. This can be achieved by ac fields with a certain ratio between driving amplitude and frequency. Since the effective amplitude depends on the difference of the qubits' Zeeman energies, a proper sequence of these energies temporarily suppresses for each qubit the interaction with exactly one of its two neighbors. After half a

tunnel cycle, the field amplitude is switched, such that the suppression is active for the connection to the other neighbor. As a consequence, the qubit is transported into one particular direction. A main benefit of this mechanism is that it does not rely on the local control of interaction parameters but only on the less demanding application of proper ac fields.

In the T-shaped configuration under investigation, one partner of an entangled pair is first routed to the node that connects Alice with Bob and Charlie. When the qubit arrives at the node, the further propagation depends on which branch is temporarily closed at that very moment. In particular, we demonstrated that for a proper phase of the driving field, the qubit is reliably routed toward the one or the other direction. The achievable entanglement increases with the driving frequency. For an idealized chain of 100 qubits with realistic parameters, the corresponding concurrence may assume values of the order 0.98.

In an experiment, however, the setup and the operation will not be ideal. Therefore, we have investigated two limiting influences, namely, fabrication imperfections of the desired splitting sequence and the influence of external degrees of freedom which lead to decoherence. The former reduce the achievable fidelity, in particular for high driving frequencies, i.e., in the regime in which the idealized model works

almost perfectly. The numerical simulation revealed the existence of an intermediate frequency regime, in which realistic fabrication errors do not significantly reduce the achievable fidelity.

The second limitation leads to the ubiquitous decoherence which generally represents the main obstacle for the implementation of quantum information schemes. It turned out that dephasing does not limit the entanglement or state transfer as long as its rate is roughly three orders of magnitude smaller than the typical qubit splitting.

In summary, we have demonstrated that the proposed quantum router should work under realistic conditions such as fabrication uncertainties and decoherence. The implementation is feasible not only with ion chains but with practically all interacting qubit arrays in a T-shaped configuration. Thus our quantum router may represent an essential building block in future quantum information networks.

[1] D. Deutsch, Proc. R. Soc. London, Ser. A **400**, 97 (1985).

[2] R. Ursin *et al.*, Nat. Phys. **3**, 481 (2007).

[3] S. Bose, Phys. Rev. Lett. **91**, 207901 (2003).

[4] S. Bose, Contemp. Phys. **48**, 13 (2007).

[5] M. Christandl, N. Datta, A. Ekert, and A. J. Landahl, Phys. Rev. Lett. **92**, 187902 (2004).

[6] G. M. Nikolopoulos, D. Petrosyan, and P. Lambropoulos, Europhys. Lett. **65**, 297 (2004).

[7] C. Di Franco, M. Paternostro, and M. S. Kim, Phys. Rev. Lett. **101**, 230502 (2008).

[8] L.-A. Wu, A. Miranowicz, X. Wang, Y.-X. Liu, and F. Nori, Phys. Rev. A **80**, 012332 (2009).

[9] A. Kay, e-print arXiv:0903.4274.

[10] C. Di Franco, M. Paternostro, D. I. Tsomokos, and S. F. Huelga, Phys. Rev. A **77**, 062337 (2008).

[11] O. Romero-Isart and J. J. García-Ripoll, Phys. Rev. A **76**, 052304 (2007).

[12] A. O. Niskanen, K. Harrabi, F. Yoshihara, Y. Nakamura, S. Lloyd, and J. S. Tsai, Science **316**, 723 (2007).

[13] S. H. W. van der Ploeg, A. Izmalkov, A. M. van den Brink, U. Hübner, M. Grajcar, E. Il'ichev, H.-G. Meyer, and A. M. Zagoskin, Phys. Rev. Lett. **98**, 057004 (2007).

[14] M. Mariantoni, F. Deppe, A. Marx, R. Gross, F. K. Wilhelm, and E. Solano, Phys. Rev. B **78**, 104508 (2008).

[15] J. You and F. Nori, Phys. Today **58**(11), 42 (2005).

[16] F. Grossmann, T. Dittrich, P. Jung, and P. Hänggi, Phys. Rev. Lett. **67**, 516 (1991).

[17] F. Grossmann and P. Hänggi, Europhys. Lett. **18**, 571 (1992).

[18] M. Grifoni and P. Hänggi, Phys. Rep. **304**, 229 (1998).

[19] V. M. Kenkre and S. Raghavan, J. Opt. B: Quantum Semiclassical Opt. **2**, 686 (2000).

[20] G. Platero and R. Aguado, Phys. Rep. **395**, 1 (2004).

[21] S. Longhi, Phys. Rev. B **77**, 195326 (2008).

[22] S. Kohler, J. Lehmann, and P. Hänggi, Phys. Rep. **406**, 379 (2005).

[23] Y. Kayanuma and K. Saito, Phys. Rev. A **77**, 010101(R) (2008).

[24] S. Camalet, J. Lehmann, S. Kohler, and P. Hänggi, Phys. Rev. Lett. **90**, 210602 (2003).

[25] C. E. Creffield, Phys. Rev. Lett. **99**, 110501 (2007).

[26] S. G. Schirmer, I. C. H. Pullen, and P. J. Pemberton-Ross, Phys. Rev. A **78**, 062339 (2008).

[27] A. Kay and P. J. Pemberton-Ross, e-print arXiv:0905.4070.

[28] D. Burgarth, K. Maruyama, M. Murphy, S. Montangero, T. Calarco, F. Nori, and M. B. Plenio, e-print arXiv:0905.3373; D. Burgarth, K. Maruyama, and F. Nori, Phys. Rev. A **79**, 020305 (2009).

[29] D. Burgarth, Ph.D. thesis, University College London, 2006.

[30] G. M. Nikolopoulos, Phys. Rev. Lett. **101**, 200502 (2008).

[31] M.-H. Yung, e-print arXiv:0705.1560.

[32] G. Ciaramicoli, I. Marzoli, and P. Tombesi, Phys. Rev. Lett. **91**, 017901 (2003).

[33] S. Stahl, F. G. J. Alonso, S. Djekic, W. Quint, T. Valenzuela, J. Verdu, M. Vogel, and G. Werth, Eur. Phys. J. D **32**, 139 (2005).

[34] F. Helmer, M. Mariantoni, A. G. Fowler, J. von Delft, E. Solano, and F. Marquardt, EPL **85**, 50007 (2009).

[35] M. B. Plenio, J. Hartley, and J. Eisert, New J. Phys. **6**, 36 (2004).

[36] G. Della Valle, M. Ornigotti, E. Cianci, V. Foglietti, P. Laporta,

and S. Longhi, Phys. Rev. Lett. **98**, 263601 (2007).

[37] C. H. Bennett, G. Brassard, C. Crepeau, R. Jozsa, A. Peres, and W. K. Wootters, Phys. Rev. Lett. **70**, 1895 (1993).

[38] H. Wichterich and S. Bose, Phys. Rev. A **79**, 060302(R) (2009).

[39] F. Galve, D. Zueco, S. Kohler, E. Lutz, and P. Hänggi, Phys. Rev. A **79**, 032332 (2009).

[40] R. D. Astumian and P. Hänggi, Phys. Today **55**(11), 33 (2002).

[41] P. Hänggi and F. Marchesoni, Rev. Mod. Phys. **81**, 387 (2009).

[42] W. K. Wootters, Phys. Rev. Lett. **80**, 2245 (1998).

[43] D. Leibfried, R. Blatt, C. Monroe, and D. Wineland, Rev. Mod. Phys. **75**, 281 (2003).

[44] C. F. Roos, D. Leibfried, A. Mundt, F. Schmidt-Kaler, J. Eschner, and R. Blatt, Phys. Rev. Lett. **85**, 5547 (2000).

[45] A. O. Caldeira and A. L. Leggett, Ann. Phys. (N.Y.) **149**, 374 (1983).

[46] V. B. Magalinskiĭ, Sov. Phys. JETP **9**, 1381 (1959).

[47] P. Hänggi and G.-L. Ingold, Chaos **15**, 026105 (2005).

[48] K. Blum, *Density Matrix Theory and Applications*, 2nd ed. (Springer, New York, 1996).

[49] G. Lindblad, Commun. Math. Phys. **48**, 119 (1976).

[50] R. Doll, D. Zueco, M. Wubs, S. Kohler, and P. Hänggi, Chem. Phys. **347**, 243 (2008).

[51] C. Roos, T. Zeiger, H. Rohde, H. C. Nägerl, J. Eschner, D. Leibfried, F. Schmidt-Kaler, and R. Blatt, Phys. Rev. Lett. **83**, 4713 (1999).

[52] R. Doll, M. Wubs, P. Hänggi, and S. Kohler, Phys. Rev. B **76**, 045317 (2007).